



Prediction of cognitive and motor development in preterm children using exhaustive feature selection and cross-validation of near-term white matter microstructure

Kornél Schadt^{a,c}, Rachel Vassar^{a,c}, Katelyn Cahill-Rowley^{a,b}, Kristen W. Yeom^d, David K. Stevenson^e, Jessica Rose^{a,b,c,*}

^a Department of Orthopaedic Surgery, Stanford University School of Medicine, Stanford, CA, United States

^b Motion & Gait Analysis Lab, Lucile Packard Children's Hospital, Stanford, CA, United States

^c Neonatal Neuroimaging Research Lab, Stanford University School of Medicine, Stanford, CA, United States

^d Department of Radiology, Lucile Packard Children's Hospital, Stanford University School of Medicine, Stanford, CA, United States

^e Division of Neonatal and Developmental Medicine, Stanford University School of Medicine, Stanford, CA, United States

ARTICLE INFO

Keywords:

MRI
DTI
Diffusion tensor imaging
Neonate
Preterm
Very-low-birth-weight
VLBW
Machine learning
Neurodevelopment
BSID
Cognitive development
Motor development

ABSTRACT

Background: Advanced neuroimaging and computational methods offer opportunities for more accurate prognosis. We hypothesized that near-term regional white matter (WM) microstructure, assessed on diffusion tensor imaging (DTI), using exhaustive feature selection with cross-validation would predict neurodevelopment in preterm children.

Methods: Near-term MRI and DTI obtained at 36.6 ± 1.8 weeks postmenstrual age in 66 very-low-birth-weight preterm neonates were assessed. 60/66 had follow-up neurodevelopmental evaluation with Bayley Scales of Infant-Toddler Development, 3rd-edition (BSID-III) at 18–22 months. Linear models with exhaustive feature selection and leave-one-out cross-validation computed based on DTI identified sets of three brain regions most predictive of cognitive and motor function; logistic regression models were computed to classify high-risk infants scoring one standard deviation below mean.

Results: Cognitive impairment was predicted (100% sensitivity, 100% specificity; AUC = 1) by near-term right middle-temporal gyrus MD, right cingulate-cingulum MD, left caudate MD. Motor impairment was predicted (90% sensitivity, 86% specificity; AUC = 0.912) by left precuneus FA, right superior occipital gyrus MD, right hippocampus FA. Cognitive score variance was explained (29.6%, cross-validated $R^2 = 0.296$) by left posterior-limb-of-internal-capsule MD, Genu RD, right fusiform gyrus AD. Motor score variance was explained (31.7%, cross-validated $R^2 = 0.317$) by left posterior-limb-of-internal-capsule MD, right parahippocampal gyrus AD, right middle-temporal gyrus AD.

Conclusion: Search in large DTI feature space more accurately identified neonatal neuroimaging correlates of neurodevelopment.

1. Introduction

At near-term age the infant brain undergoes rapid growth and microstructural development (Brody et al., 1987; Dubois et al., 2006; Huang et al., 2006; Kinney et al., 1988; Nossin-Manor et al., 2013; Oishi et al., 2011; Rose et al., 2014). Brain microstructure abnormalities assessed at this age are plausible prognostic factors of neurodevelopment in preterm children (Aeby et al., 2013; Alvarez et al., 2011; Arzoumanian et al., 2003; Mukherjee et al., 2002; Rose et al., 2015, 2009, 2007; Van Kooij et al., 2011; Woodward et al., 2012). Although

advances in neonatal medicine have increased the survival rate and positive outcome among children born preterm, 40–50% of very preterm infants still experience neurodevelopmental impairments such as cerebral palsy (CP), developmental coordination disorder, as well as cognitive and language delay (Spittle et al., 2011; Williams et al., 2010). CP affects 10–15% of very-low-birth-weight (VLBW) preterm children compared to 0.3% of children born full-term; among extremely preterm infants, cognitive and motor delay occurs in 33% and 18%, respectively, compared to 13% and 1% in children born full-term (Woodward et al., 2012).

* Corresponding author at: Department of Orthopaedic Surgery, Stanford University School of Medicine, Stanford, CA, United States.
E-mail address: jessica.rose@stanford.edu (J. Rose).

At term-equivalent age, reduction in cerebral volume and white matter (WM) immaturity has been reported in preterm infants compared to full-term neonates (Hüppi et al., 1998; Inder et al., 2005; Lee et al., 2013; Rose et al., 2008; Thompson et al., 2013, 2006). Neonatal neuroimaging holds potential for identifying early biomarkers of neurodevelopmental impairment to guide early intervention at a time of optimal neuroplasticity and rapid cognitive and motor development.

Diffusion tensor imaging (DTI) measures water diffusion in multiple directions. The movement of water molecules is restricted by cellular barriers (e.g. cellular membranes or axonal myelination where present), thus DTI can be used to obtain information about underlying tissue organization (Basser and Pierpaoli, 2011; Counsell et al., 2002; Hüppi et al., 1998; Pierpaoli et al., 1996). DTI quantifies fractional anisotropy (FA), mean diffusivity (MD), radial diffusivity (RD), and axial diffusivity (AD). FA is a scalar between 0 and 1 that expresses the degree of restriction that limits diffusion to a distinct direction (Pierpaoli et al., 1996), in WM it is altered by fiber coherence, diameter, density, and myelination. MD is the average displacement of water molecules, AD is the displacement along the primary axis, and RD is the displacement perpendicular to the primary axis.

Brain development involves certain processes that change the dynamics of diffusion, e.g. decreased water content, contraction of extracellular space, myelination, and increased coherence of axonal structures (Dubois et al., 2008; Kinney et al., 1994; Nossin-Manor et al., 2013). FA, MD, AD, and RD values are affected by these changes and can assess brain development and maturation.

VLBW preterm infants typically undergo standard-of-care neuroimaging prior to discharge from the neonatal intensive care unit. Determining prognostic biomarkers on conventional structural brain MRI scans have been reported (Hintz et al., 2015; Miller and Ferriero, 2009). Employing DTI is a promising extension of neuroimaging techniques to assess early WM microstructure and may improve the overall prognostic accuracy for developmental outcomes (Arzoumanian et al., 2003; Rose et al., 2015, 2009, 2007).

Previously we reported neurodevelopmental outcome in relation to near-term regional WM assessed on DTI in 6 subcortical WM regions (4 bilateral regions, 2 regions of the corpus callosum) selected based on functional relevance, in the same cohort of VLBW preterm children, using standard statistical techniques (Rose et al., 2015). In contrast, the current study employs statistical learning approaches with exhaustive feature selection and leave-one-out cross-validation of 51 WM regions (48 bilateral regions, 3 regions of corpus callosum) to investigate utilizing DTI based multivariate linear models in the NICU for early prognosis. Search in large feature space may more accurately identify neonatal neural correlates of neurodevelopmental delay, and ultimately inform neuroprotective treatment to improve quality of life for preterm children. Here we use a statistical learning approach to examine near-term WM microstructure in VLBW preterm neonates in relation to cognitive and motor outcome at 18–22 months adjusted age. We hypothesized that WM microstructure in a subset of three near-term brain regions, identified using statistical learning approach of exhaustive feature selection and cross-validation, would demonstrate higher predictive value for cognitive and motor development at 18–22 month of adjusted age, compared to using standard techniques.

Our analysis utilized machine learning applied to linear models using a standard exhaustive feature search and cross-validation. Exhaustive feature search is an optimal feature selection method that is employed when the size of dataset and the number of required features allow the exhaustive feature selection to be computation feasible (Wang et al., 2016). Cross-validation is the most widely-used technique to estimate generalization capability and prediction error of a machine learning model (Hastie et al., 2009).

This approach was selected for its simplicity of design, generalization capability, and potential for use in other cohorts and clinical applications.

2. Methods

Participants were selected based on criteria of gestational age at birth ≤ 32 weeks, VLBW (birth weight ≤ 1500 g), and absence of evidence of genetic disorder or congenital brain abnormalities. 102 infants treated at Lucile Packard Children's Hospital (LPCH) from 1/1/10–12/31/11 participated, representing 76% of eligible infants who were admitted to the NICU over the two-year period. Parents were approached prior to scheduled routine MRI and consent was obtained for this IRB-approved study. 66 of the 102 neonates had successful DTI scans, collected at the end of routine MRI scan, prior to discharge.

Of the 66 neonates who had both near-term MRI and DTI, 60 returned for follow-up neurodevelopmental assessment at 18–22 months; 59 completed cognitive BSID-III, and 60 completed motor BSID-III. Cognitive and motor development was assessed using the BSID-III composite cognitive and motor scores, as well as fine motor and gross motor sub-scores of BSID-III, adjusted for age, as previously described (Rose et al., 2015).

2.1. MRI data acquisition

Brain MRI scans were performed on 3 T MRI (GE Discovery MR750, GE 8-Channel HD head coil, Little Chalfont, UK) at LPCH. A 3-plane localizer was used, and an asset calibration was prescribed to utilize parallel imaging. Sagittal T1 FLAIR image parameters were: TE = 91.0, TR = 2200, FOV = 20 cm, matrix size = 320×224 , slice thickness 3.0×0.5 mm spacing, NEX = 1. T2, DWI, and DTI axial scans were prescribed using a single acquisition, full-phase field of view (FOV). The axial fast spin echo T2 imaging parameters were: TE = 85 ms, TR = 2500, FOV = 20 cm, matrix = 384×224 ; slice = $4.0 \text{ mm} \times 0.0$ mm spacing. Axial T2 FLAIR parameters were: TE = 140, TR = 9500, FOV = 20 cm, slice = $4.0 \text{ mm} \times 0.0$ mm, inversion time = 2300, fluid attenuated inversion recovery matrix = 384×224 . Axial DWI parameters were: TE = 88.8, TR = 10,000, FOV = 20 cm, slice = $4.0 \text{ mm} \times 0.0$ mm spacing, matrix = 128×128 . Coronal T1 SPGR parameters were: TE = 8, TR = 3, slice = $1.0 \text{ mm} \times 0.0$ spacing, FOV = 24 cm, matrix = 256×256 .

2.2. Radiological assessment

Structural MRI was assessed for degree of WMA and significant cerebellar abnormality. Radiological evaluation was performed by an experienced pediatric neuroradiologist (X.S.) and confirmed by a second (K.Y.), both were masked to all other participant data. A form validated for near-term neuroradiological assessment (Hintz et al., 2015) was used to score WMA (1–3) according to a widely used classification system (Hintz et al., 2015; Horsch et al., 2010; Woodward et al., 2006): (i) extent of WM signal abnormality, (ii) periventricular WM volume loss, (iii) cystic abnormalities, (iv) ventricular dilation, and (v) thinning of the CC. High inter-rater agreement (96%–98%) for moderate-severe WMA using this classification was reported (Hintz et al., 2015; Woodward et al., 2006). Significant cerebellar abnormalities included significant cerebellar lesions defined by Hintz et al. and/or significant cerebellar asymmetry of ≥ 3 mm in the anterior-posterior or medial-lateral direction (Hintz et al., 2015).

DTI was calculated based on diffusion weighted images (DWI) obtained along 25 orientations with slice thickness of 3 mm, matrix size of 128×128 , and 90-degree flip angle on a 3 T MRI (GE Discovery MR750, GE 8-Channel HD head coil) at LPCH at the end of routine MRI acquisition. A repetition of DTI sequence was successfully collected in 64 of 66 cases. Infants were swaddled and fed, and typically remained asleep during the scan. Sedation typically was not utilized for routine near-term MRI, and was not utilized as part of the research protocol.

2.3. DTI processing

To eliminate images with artifacts or evidence of motion, the best DTI repetitions were selected by a trained inspector. In 2 of 66 cases, no full repetition was usable, therefore a composite repetition was generated from the best image slices. Affine transformation was applied to correct eddy current distortions. Skull stripping was performed based on B0 and trace (vectorial sum of diffusivity) maps using ROI editor, and manually rotated to align the JHU neonatal template. Scans were analyzed using DTI-studio with settings detailed in Oishi et al., in a semi-automated, atlas based manner (Oishi et al., 2011). DTI images were processed using DiffeoMap using FA and trace map to perform a large deformation diffeomorphic metric mapping transformation (Oishi et al., 2011). Amplitude of trace $> 0.006 \text{ mm}^2/\text{s}$ and FA < 0.15 were considered cerebrospinal fluid (CSF) and gray matter, respectively, and were used to obtain the mask of WM regions. WM regions were then segmented into 126 regions based on the JHU parcellation atlas, and the average FA, MD, AD, and RD values were calculated for each region. The number of regions were then narrowed to apical regions ensuring the quality of registration, resulting in 48 regions of both sides in addition to the splenium and genu of the corpus callosum (CC), and the overall CC. Further examination was performed on the FA, MD, AD, and RD values of a total of 99 regions adjusted for post menstrual age (PMA) at scan.

2.4. Statistical analysis

Correlations between DTI measures and BSID-III scores were analyzed using distinct linear models generated for cognitive composite, motor composite, fine motor, and gross motor scores. Using an exhaustive search in the feature space, multivariate linear regression models were evaluated to find a set of 3 regions (features) most correlated with BSID-III scores. Logistic regression models were evaluated on DTI to find a set of 3 regions that best classified high-risk infants scoring below one standard deviation below mean. Best models were selected based on cross-validated coefficient of determination (R^2) for linear regression, and cross-validated area under the curve (AUC) of the receiver operator characteristic (ROC) for the binary classification with logistic regression.

DTI scalars were adjusted for PMA at scan and normalized to have zero mean and unit variance. To ensure model generalization and robustness, and avoid overfitting, performance measures, such as R^2 and AUC, were evaluated with leave-one-out cross-validation (LOOCV). For the classification tasks (high-risk vs. low-risk), 3 thresholds on the logistic functions were evaluated: (i) to obtain balanced sensitivity and specificity determined by maximizing the sum of the squares of sensitivity and specificity ($\text{sensitivity}^2 + \text{specificity}^2$), (ii) specificity given the maximum achievable sensitivity, and (iii) sensitivity given the maximum achievable specificity (Table 2b, 3b, 4b, 5b). The balanced sensitivity and specificity are reported in the text. Results were obtained using Scikit-learn (Pedregosa et al., 2011) and Statsmodels (Seabold and Perktold, 2010).

Non-image clinical features – including gender, gestational age, birth weight, small for gestational age, multiple births, presence of bronchopulmonary dysplasia and necrotizing enterocolitis, stage of retinopathy of prematurity (ROP), and average serum CRP and albumin over the first 2 weeks of life as previously defined (Rose et al., 2015) – were also evaluated using exhaustive feature selection, cross-validation, and logistic regression to compare their predictive performance to DTI-based predictions.

3. Results

Table 1 reports neonatal clinical characteristics as well as classification of high risk infants using logistic regression with exhaustive feature selection and cross-validation based on near-term DTI and on

near-term structural MRI findings, in VLBW preterm children who scored $< \text{one SD}$ versus $\geq \text{one SD}$ below mean BSID-III cognitive and motor score, at 18–22 months of adjusted age.

Cognitive impairment based on BSID-III cognitive composite score was correctly classified using logistic regression on near-term DTI with exhaustive feature selection and cross-validation (100% sensitivity, 100% specificity, AUC = 1) based on near-term WM microstructure in three brain regions: right middle temporal gyrus MD, right cingulate gyrus part of the cingulum MD, and left caudate nucleus MD (Table 2b; Fig. 1a and b). The same statistical approach using structural brain MRI findings of WMA score, presence of cerebellar signal abnormality, and cerebellar asymmetry, classified infants with cognitive impairment with lower accuracy (50% sensitivity, 80% specificity, AUC = 0.582). The 3 most predictive non-image clinical features were gestational age, multiple birth, and presence of bronchopulmonary dysplasia (72% sensitivity, 73% specificity, AUC = 0.707).

Cognitive composite score was predicted using linear regression on near-term DTI with exhaustive feature selection and cross-validation ($R^2 = 0.375$, adjusted $R^2 = 0.341$, cross-validated $R^2 = 0.296$) based on near-term WM microstructure in three brain regions: left PLIC MD, Genu RD, and right fusiform gyrus AD, which explained 29.6% of variance of BSID-III cognitive composite score at 18–22 months of age (Table 2a).

Motor impairment based on BSID-III motor composite score of preterm children was correctly classified using logistic regression on near-term DTI with exhaustive feature selection and cross-validation (90% sensitivity, 86% specificity, AUC = 0.912) based on near-term WM microstructure in three brain regions: by left precuneus FA, right superior occipital gyrus MD, right hippocampus FA (Table 3b; Fig. 2a and b). The same statistical approach using structural brain MRI findings of WMA score, presence of cerebellar signal abnormality, and cerebellar asymmetry, classified infants with cognitive impairment with lower accuracy (60% sensitivity, 53.7% specificity, AUC = 0.367). The 3 most predictive non-image clinical features were gestational age, multi birth, stage of ROP (70% sensitivity, 72% specificity, AUC = 0.699).

Motor composite score was predicted using linear regression on near-term DTI with exhaustive feature selection and cross-validation ($R^2 = 0.401$, adjusted $R^2 = 0.369$, cross-validated $R^2 = 0.317$) based on near-term WM microstructure in three brain regions: left PLIC MD, right parahippocampal gyrus AD, and right middle temporal gyrus AD, which explained 32% of variance of BSID-III cognitive composite score at 18–22 months of age (Table 3a).

Fine motor development was correctly classified using logistic regression on near-term DTI with exhaustive feature selection and cross-validation (100% sensitivity, 87.8% specificity, AUC = 0.957) based on near-term WM microstructure in three brain regions: right stria terminalis FA, left inferior occipital gyrus MD, and right superior parietal gyrus MD (Table 4b; Fig. 3a and b). The same statistical approach using structural brain MRI findings of WMA score, presence of cerebellar signal abnormality, and cerebellar asymmetry, classified infants with cognitive impairment with lower accuracy (73% sensitivity, 56% specificity, AUC = 0.418). The 3 most predictive non-image clinical features were average serum CRP level over the first two weeks of life, stage of ROP, presence of bronchopulmonary dysplasia (82% sensitivity, 60% specificity, AUC = 0.646).

Fine motor subscore was predicted using linear regression on near-term DTI with exhaustive feature selection and cross-validation ($R^2 = 0.351$, adjusted $R^2 = 0.316$, cross-validated $R^2 = 0.268$) based on near-term WM microstructure in three brain regions: right superior parietal gyrus AD, left superior frontal gyrus MD, and right supramarginal gyrus FA, which explained 26.8% of variance of BSID-III fine motor subscore at 18–22 months of age (Table 4a).

Gross motor impairment was correctly classified using logistic regression on near-term DTI with exhaustive feature selection and cross-validation (93.3% sensitivity, 66.7% specificity, AUC = 0.84) based on

Table 1

Clinical characteristics and classification using logistic regression with exhaustive feature selection and cross-validation of near-term DTI compared to near-term structural MRI findings, in VLBW preterm children who scored below one SD ($< 1SD$) versus equal to or greater than one SD ($\geq 1SD$) below mean BSID-III cognitive and motor score. MRI findings include presence of white matter abnormality (WMA), cerebellar signal abnormality, and cerebellar asymmetry.

	BSID-III cognitive composite		BSID-III motor composite		BSID-III fine motor		BSID-III gross motor	
	$< 1SD$	$\geq 1SD$	$< 1SD$	$\geq 1SD$	$< 1SD$	$\geq 1SD$	$< 1SD$	$\geq 1SD$
Total (N)	8	51	10	50	11	49	15	45
GA-at-birth (days, mean [SD])	187.75 [13.27]	203.22 [16.07]	196.10 [15.81]	202.44 [16.52]	199.64 [16.82]	201.78 [16.49]	197.87 [17.24]	202.56 [16.17]
Birth weight (g, mean [SD])	925.00 [247.02]	1089.51 [261.72]	1021.80 [271.13]	1075.14 [261.27]	985.73 [268.21]	1084.33 [259.25]	1006.73 [303.12]	1086.09 [245.98]
PMA-at-scan (g, mean [SD])	258.50 [9.07]	255.69 [9.01]	254.20 [6.85]	256.24 [9.44]	255.00 [10.25]	256.10 [8.79]	257.33 [9.29]	255.42 [8.97]
Prediction using DTI-based logistic regression with LOOCV	8/8	51/51	8/10	48/50	11/11	43/49	14/15	30/45
Prediction using WMA identified on structural MRI (N/total)	0/8	47/51	1/10	47/50	0/11	45/49	1/15	42/45
Prediction using cerebellar signal abnormality identified on structural MRI (N/total)	2/8	45/51	2/10	44/50	2/11	43/49	3/15	40/45
Prediction using cerebellar asymmetry identified on structural MRI (N/total)	1/8	47/51	1/10	46/50	0/11	44/49	1/15	41/45

near-term WM microstructure in three brain regions: left lingual gyrus FA, right parahippocampal gyrus MD, and right gyrus rectus AD (Table 5b; Fig. 4a and b). The same statistical approach using structural brain MRI findings of WMA score, presence of cerebellar signal abnormality, and cerebellar asymmetry, classified infants with cognitive impairment with lower accuracy (26% sensitivity, 78% specificity, AUC = 0.333). The 3 most predictive non-image clinical features were gender, multiple birth, and average serum albumin level over the first two weeks of life (58% sensitivity, 76% specificity, AUC = 0.647).

Gross motor subscore was predicted using linear regression on near-term DTI with exhaustive feature selection and cross-validation ($R^2 = 0.393$, adjusted $R^2 = 0.361$, cross-validated $R^2 = 0.284$) based on near-term WM microstructure in three brain regions: left PLIC MD, right precentral gyrus FA, and right parahippocampal gyrus AD, which explained 28% of variance of BSID-III gross motor subscore at 18–22 months of age (Table 5a).

4. Discussion

The statistical learning method of exhaustive feature search and LOOCV was applied to examine prediction based on near-term brain microstructure assessed on DTI in relation to cognitive and motor development in preterm toddlers at 18–22 months adjusted age. These results were compared with models using structural MRI findings. Classification of infants at high-risk for cognitive impairment was predicted by near-term WM in right middle temporal gyrus MD, right cingulate gyrus part of the cingulum MD, and left caudate nucleus MD, with 100% sensitivity and 100% specificity. Cognitive composite score was predicted by near-term WM microstructure in three brain regions: left PLIC MD, Genu RD, and right fusiform gyrus AD, which explained 30% of variance of preterm children at 18–22 months adjusted age. Classification of infants at high-risk for motor impairment was predicted by near-term by left precuneus FA, right superior occipital gyrus MD, right hippocampus FA with 90% sensitivity and 86% specificity, and with the same AUC by right inferior fronto-occipital fasciculus AD, left caudate nucleus FA, and left fusiform gyrus FA, with 80% sensitivity and 96% specificity. Motor composite score was predicted by near-term WM in left PLIC MD, right parahippocampal gyrus AD, and right middle temporal gyrus AD, which explained 32% of variance. Statistical learning, an area of machine learning, has been successfully applied to fields such as security and insurance, to assess risk, and is a promising method to improve prognostic accuracy and guide early treatment of preterm infants. Due to the multiple comparison inherent

to exhaustive search, LOOCV was applied to reduce overfitting and optimize robustness of generalization. Application of this exhaustive feature search statistical learning approach generated relatively high predictive values, compared to standard techniques and prior studies of neuroimaging at near-term age.

Rose et al. reported data from the same cohort as the current study, and evaluated neonatal physiological risk factors, WMA assessed on structural MRI, and 6 subcortical WM regions assessed on DTI, using a standard hypothesis-driven, multivariate regression model (Rose et al., 2015). These prior results indicated that a model including left PLIC MD, genu MD, presence of cerebellar abnormality, mean serum c-reactive protein (CRP), and sepsis during the first two weeks of life significantly predicted BSID-III cognitive composite score, explaining 25% of the variance (adjusted $R^2 = 0.247$, $df = 5$). A multivariate regression model that included the left PLIC MD, and BPD significantly predicted BSID-III motor score, explaining 13% of variance (adjusted $R^2 = 0.131$, $df = 2$). In contrast, the current study evaluated all brain WM regions that were well assessed on DTI at near-term age, and did not include clinical biomarkers in the model. Using the more comprehensive statistical learning approach, the set of most predictive regions explained 30% of the variance of cognitive and 32% of the variance of motor development. Prediction based on structural MRI findings, and also on non-image clinical features were assessed separately, employing the same method. Results of the statistical learning models using the three distinct feature sets (DTI vs. structural MRI vs. non-image clinical features) indicate that models utilizing DTI offer more robust prediction.

Prior studies, such as Drobyshevsky et al. also found correlation between PLIC FA in preterm infants at 30 weeks GA and neurodevelopment at 2 years adjusted age (Drobyshevsky et al., 2007). De Bruine et al. assessed PLIC microstructure using DTI tractography at term equivalent age in relation to cognitive and motor development in very preterm toddlers and found that PLIC FA predicted motor delay (AUC = 0.89) (Bruine et al., 2013). Nagy et al. showed that prematurity-related neonatal microstructural abnormalities in the PLIC were evident on DTI at long-term follow-up of age 11 (Nagy et al., 2003). Tsao et al. also reported reduced WM integrity of corticospinal projections in the PLIC, assessed on DTI in adolescents with congenital hemiparesis (Tsao et al., 2014). Vanberg et al. studied DTI in teenagers born VLBW preterm and reported reduced WM integrity in the PLIC (Vangberg et al., 2006). These studies report consistent findings of reduced PLIC WM integrity and suggest that near-term DTI findings may persist and contribute to long-term impairment of cognitive and motor

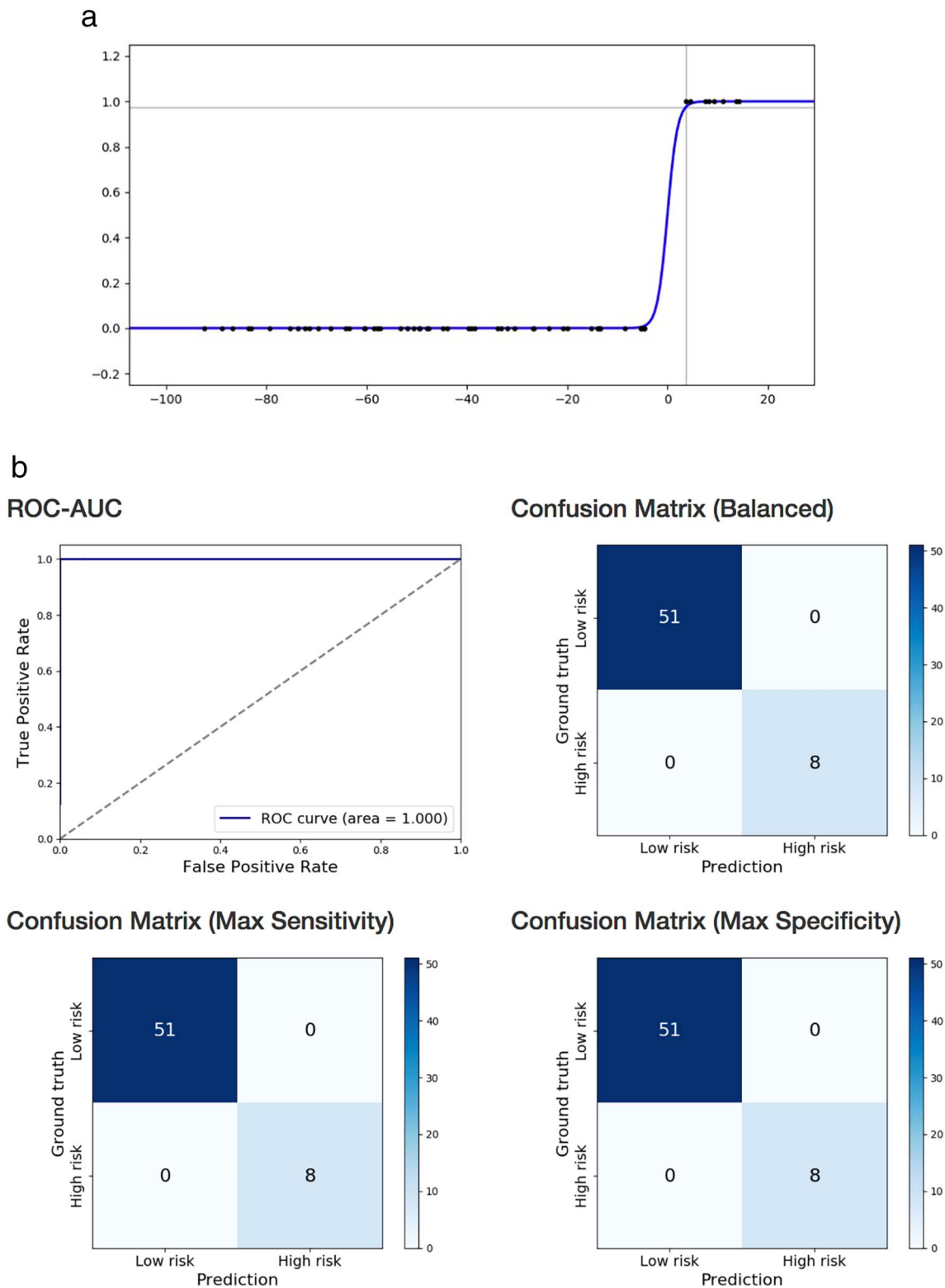


Fig. 1. a. Prediction of BSID-III cognitive composite score below one standard deviation of mean in preterm children at 18–22 months, based on near-term DTI using logistic regression. Logistic function fitted on right middle temporal gyrus MD, right cingulate gyrus part of the cingulum MD, and left caudate nucleus MD. Score below one standard deviation of the mean denoted by 1 on the y axis.

b. Prediction of BSID-III cognitive composite score below one standard deviation of mean in preterm children at 18–22 months, based on near-term DTI using logistic regression. Receiver operating characteristics curve and confusion matrices of cross-validated classification of VLBW preterm infants at high-risk for cognitive impairment from right middle temporal gyrus MD, right cingulate gyrus part of the cingulum MD, and left caudate nucleus MD.

Table 2a

Prediction of BSID-III cognitive composite score in VLBW preterm children at 18–22 months of age based on near-term white matter microstructure assessed on DTI, using exhaustive feature selection with leave-one-out cross-validation and linear regression. The five most predictive set of three brain regions are listed.

Regions	R ²	Adj. R ²	LOOCV R ²
L PLIC MD Genu RD R fusiform gyrus AD	0.375	0.341	0.296
L PLIC MD L ALIC MD L lateral orbitofrontal AD	0.354	0.319	0.275
L PLIC MD L ALIC MD L lateral orbitofrontal MD	0.354	0.318	0.274
L PLIC RD Genu RD R fusiform gyrus AD	0.349	0.313	0.267
L PLIC MD L ALIC AD L lateral orbitofrontal MD	0.344	0.309	0.263

function.

Specifically, we found that 30% of BSID-III cognitive composite score variance was explained by PLIC MD, along with genu RD, and right fusiform gyrus AD, and that 32% of motor score variance was explained by left PLIC MD, right parahippocampal gyrus AD, and right middle temporal gyrus AD. Woodward and Inder et al. examined 104 preterm and 107 full-term infants and found that reduced myelination of the corpus callosum assessed on near-term MRI was associated with IQ evaluated at ages 4 and 6 years ($r = -0.24$ and -0.28 , $p < 0.02$) (Woodward et al., 2012). Rose SE et al. examined 23 preterm infants and found reduced FA mainly within the posterior regions of the corpus callosum (Rose et al., 2008). Genu WM microstructure was reported previously to play an important role in working memory at infancy (Short et al., 2013) and IQ (Kontis et al., 2009). In addition to WM findings in the PLIC and corpus callosum, prior studies predicting outcome in preterm infants found significant associations with cortical WM. Krishnan et al. studied 38 preterm infants and found apparent diffusion coefficient assessed on DTI at term equivalent age at the level of centrum semiovale demonstrated significant negative correlation with developmental scores at 2 years follow up (Krishnan et al., 2007). Isaacs et al. studied preterm children and found that fusiform gyrus gray matter thickness assessed with volume-based morphometry had significant negative correlation with IQ assessed at age 7 years (Isaacs

Table 3a

Prediction of BSID-III composite motor score in VLBW preterm children at 18–22 months of age based on near-term white matter microstructure assessed on DTI, using exhaustive feature selection with leave-one-out cross-validation and linear regression. The five most predictive set of three brain regions are listed.

Regions	R ²	Adj. R ²	LOOCV R ²
L PLIC MD R parahippocampal gyrus AD R middle temporal gyrus AD	0.401	0.369	0.317
L PLIC MD R parahippocampal gyrus AD R supramarginal gyrus FA	0.389	0.356	0.31
L PLIC MD L ALIC RD R supramarginal gyrus FA	0.378	0.344	0.305
L PLIC MD R parahippocampal gyrus AD R middle temporal gyrus FA	0.382	0.349	0.302
L PLIC MD R parahippocampal gyrus AD R gyrus rectus AD	0.373	0.340	0.288

et al., 2004).

The predictive value of WM microstructure assessed on DTI likely depends on (i) how well a region is captured, which can be affected by e.g. signal to noise ratio, and presence of crossing fibers, (ii) how well a region reflects overall brain development, (iii) functional relevance, (iv) stage of development. At near-term age, regional WM is rapidly developing. During the third trimester, fetal brain development goes through rapid growth and neurogenesis (Brody et al., 1987; Dobbing and Sands, 1973; Dubois et al., 2008; Huang et al., 2006; Kinney et al., 1988; Nossin-Manor et al., 2013) that may be altered as a result of preterm birth (Malik et al., 2013). During the first year of life, preterm and full-term infant brain development are similar in terms of a progressive decrease in water diffusion due to proliferation of oligodendrocytes and general WM maturation (Dubois et al., 2008; Lee et al., 2013; Serag et al., 2012). However, at term-equivalent age preterm infant brains differ from term-born neonates in reduced cerebral and cortical volumes (Inder et al., 2005; Thompson et al., 2013, 2006) and WM maturity (Hüppi et al., 1998; Lee et al., 2013; Rose et al., 2008). Brain regions undergoing pre-myelination, oligodendrocytic proliferation, and formation of axonal-glia synapses may be particularly vulnerable to hypoxic ischemia and diffuse cerebral WM injury (Liu et al., 2013) and if well captured, these regions may be predictive of later outcome and guide early treatment. For example, the trajectory of PLIC

Table 2b

Classification of VLBW preterm infants at high-risk for cognitive impairment based on near-term regional white matter microstructure assessed on DTI, using exhaustive feature selection and logistic regression for prediction of BSID-III cognitive composite score below one standard deviation of the mean in preterm children at 18–22 months. The five most predictive set of three brain regions are listed.

Regions	AUC	Balanced		Maximum sensitivity		Maximum specificity	
		Sens	Spec	Sens	Spec	Sens	Spec
R middle temporal gyrus MD R cingulate gyrus part of the cingulum MD L caudate nucleus MD	1	1	1	1	1	1	1
R inferior temporal gyrus AD L uncinate fasciculus RD R cingulate gyrus FA	0.995	1	0.98	1	0.98	0.75	1
R middle temporal gyrus MD R cingulate gyrus part of the cingulum MD L caudate nucleus RD	0.995	1	0.961	1	0.961	0.875	1
R inferior temporal gyrus AD L uncinate fasciculus RD L cingulate gyrus FA	0.993	1	0.941	1	0.941	0.875	1
R inferior temporal gyrus AD L uncinate fasciculus RD L angular gyrus FA	0.983	1	0.98	1	0.98	0.625	1

Table 3b

Classification of VLBW preterm infants at high-risk for motor impairment based on near-term regional white matter microstructure assessed on DTI, using exhaustive feature selection and logistic regression for prediction of BSID-III motor composite score below one standard deviation of the mean in the preterm children at 18–22 months. The five most predictive set of three brain regions are listed.

Regions	Balanced			Maximum sensitivity		Maximum specificity	
	AUC	Sens	Spec	Sens	Spec	Sens	Spec
L precuneus FA	0.912	0.9	0.86	1	0.82	0.2	0.98
R superior occipital gyrus MD							
R hippocampus FA							
R inf. Fronto-occipital fasc. AD	0.912	0.8	0.96	1	0.52	0.7	0.98
L caudate nucleus FA							
L fusiform gyrus FA							
R middle temporal gyrus FA	0.908	0.9	0.74	1	0.66	0.3	1
L inferior temporal gyrus FA							
L angular gyrus RD							
R inf. Fronto-occipital fasc. AD	0.902	0.9	0.88	1	0.4	0.3	0.98
L caudate nucleus FA							
L inferior temporal gyrus FA							
R inf. Fronto-occipital fasc. MD	0.894	0.9	0.82	1	0.72	0.1	1
R amygdala FA							
R hippocampus FA							

Table 4a

Prediction of BSID-III fine motor subscore in preterm children at 18–22 months of age based on near-term white matter microstructure assessed on DTI in the VLBW preterm infants, using exhaustive feature selection with leave-one-out cross-validation and linear regression. The five most predictive set of three brain regions are listed.

Regions	R ²	Adj. R ²	LOOCV R ²
R superior parietal gyrus AD	0.351	0.316	0.268
L superior frontal gyrus MD			
R supramarginal gyrus FA			
R superior parietal gyrus AD	0.336	0.301	0.256
L superior frontal gyrus AD			
R supramarginal gyrus FA			
R superior parietal gyrus MD	0.328	0.292	0.248
L superior frontal gyrus MD			
R supramarginal gyrus FA			
R superior parietal gyrus MD	0.343	0.308	0.247
L superior frontal gyrus MD			
R stria terminalis FA			
R superior parietal gyrus MD	0.330	0.294	0.246
L superior frontal gyrus RD			
R supramarginal gyrus FA			

WM myelination, which is observed histologically between 32 and 35 weeks (Cowan and De Vries, 2005) results in selective vulnerability during the third trimester. Using this exhaustive feature search with cross-validation we found that left PLIC MD consistently contributed to the top models predicting cognitive and motor outcomes.

Cognitive development at 18–22 months adjusted age was predicted by near term left ALIC and the left lateral orbitofrontal cortex in several of the top 5 models. The ALIC conveys fibers involved in higher order cognition and develops slightly later than the PLIC (Barkovich et al., 1988; Yakovlev, 1967), and therefore may also be vulnerable at pre-term age. Giménez et al. found decreased gray matter in the orbitofrontal area in adolescents with history of very preterm birth (Giménez et al., 2006). However, myelination of regional WM in the lateral orbitofrontal gyrus begins before birth and takes place gradually over

many years until adult age (Fuster, 2002). As a predictive area, it contributed to 3 out of 5 top models for cognitive development, suggesting functional relevance, and may indicate overall brain development. The orbitofrontal cortex was previously reported to play significant role in cognitive tasks at age 8–12 in typically developing children (Bunge and Wright, 2007).

Motor development at 18–22 months adjusted age was predicted by near-term PLIC MD, as well as right parahippocampal gyrus AD, and right middle temporal gyrus AD. Middle temporal gyrus mediates visual cognition and may contribute to the child's ability to plan and perform motor tasks suggesting function relevance. Parahippocampal gyrus is part of the limbic system and plays an important role in memory. Structural proximity of the parahippocampal gyrus, middle and inferior temporal gyrus, and fusiform gyrus suggests WM functional interdependence, and may reflect overall brain development.

Classification of infants at high risk for cognitive impairment was informed by cingulate gyrus, which is involved in sensorimotor function and executive control (Devinsky et al., 1995; Schmahmann et al., 2007), and contributed to 4 out of the top 5 classification models. Given the medial to peripheral trajectory of WM development in infants (Rose et al., 2014), the medial location of the cingulate gyrus may suggest sufficient maturation at near-term age. Kesler et al. previously found that there is a significant decrease in cingulate gyrus WM volume among preterm children at age 8 years compared to term born children, but by age 12, deficits in the cingulate gyrus only remained significant in males (Kesler et al., 2008, 2004).

Classification of high risk infants for cognitive and motor impairment was informed by the left caudate nucleus in 2 out of the top 5 models for both cognitive and motor score. Caudate nucleus is involved in both cognition as well as fine motor control (Finch et al., 1981; Graybiel, 2000) and begin myelination around 35–36 weeks GA (Rose et al., 2014). Snook et al. reported a steep increase in FA during childhood (Snook et al., 2005), while Mukherjee et al. found only a minor increase between age 4–12 years (Mukherjee et al., 2002). At near-term age, we found that caudate FA, MD, and RD values contributed to highly predictive models for both cognitive and motor impairment. In addition, inferior and middle temporal gyrus, known to be involved in visual cognition, semantic memory processing, and language (Cabeza and Nyberg, 2000; Chao et al., 1999; Herath et al., 2001; Ishai et al., 1999; Miyashita, 1993; Tranel et al., 1997), were predictive for classification of cognitive and motor scores. Gaillard et al. reported strong activation of fMRI signal in the middle temporal gyrus on reading tasks in typically developing children (Gaillard et al., 2001). Our results suggest near term DTI metrics in the temporal gyri may contribute to prediction of later cognitive and motor function. Classification of motor impairment with highest sensitivity was informed by left precuneus FA, right superior occipital gyrus MD, and right hippocampus FA. Precuneus was previously found to play an important role in coordination of motor behaviour, motor imagery, and mental rotation (Hanakawa et al., 2003; Suchan et al., 2002; Wenderoth et al., 2005). Hippocampus is known to be involved in procedural memory, contributing to consolidation of motor sequence memory (Albouy et al., 2008).

Prediction of the models using DTI outperformed models using structural MRI, reinforcing prior studies that found DTI might yield more sensitive predictors compared to structural MRI for neurodevelopmental outcome (Arzoumanian et al., 2003; Bruïne et al., 2013; Rose et al., 2009, 2007). Employing DTI in combination with the statistical learning approach of exhaustive feature selection and cross-validation has potential to improve prognostic accuracy of neonatal neuroimaging. Advances in automated data processing increase the clinical feasibility of using DTI, improving its ease of use, repeatability, and thus prognostic value. Logistic regression used in this study is a linear model, therefore both its implementation and interpretation is relatively straightforward. If replicated in a larger population, these methods could be implemented clinically to improve prognostic accuracy.

Table 4b

Classification of VLBW preterm infants at high-risk for fine motor impairment based on near-term regional white matter microstructure assessed on DTI, using exhaustive feature selection and logistic regression for prediction of BSID-III fine motor subscore below one standard deviation of the mean in preterm children at 18–22 months. The five most predictive set of three brain regions are listed.

Regions	AUC	Balanced		Maximum sensitivity		Maximum specificity	
		Sens	Spec	Sens	Spec	Sens	Spec
R stria terminalis FA	0.957	1	0.878	1	0.878	0.727	0.98
L inferior occipital gyrus MD							
R superior parietal gyrus MD							
R stria terminalis FA	0.954	0.909	0.918	1	0.816	0.273	1
L inferior occipital gyrus MD							
R superior parietal gyrus RD							
R stria terminalis FA	0.944	0.909	0.898	1	0.694	0.273	1
L inferior occipital gyrus RD							
L lingual gyrus MD							
R stria terminalis FA	0.942	0.909	0.837	1	0.735	0.455	1
L inferior occipital gyrus RD							
L lingual gyrus AD							
R stria terminalis FA	0.942	0.909	0.857	1	0.796	0.636	0.98
L inferior occipital gyrus RD							
R superior parietal gyrus RD							

Table 5a

Prediction of BSID-III gross motor subscore in VLBW preterm children at 18–22 months of age from near-term white matter microstructure assessed on DTI, using exhaustive feature selection with leave-one-out cross-validation and linear regression. The five most predictive set of three brain regions are listed.

Regions	R ²	Adj. R ²	LOOCV R ²
L PLIC MD	0.393	0.361	0.284
R precentral gyrus FA			
R parahippocampal gyrus AD			
L PLIC MD	0.376	0.343	0.273
L ALIC RD			
R postcentral gyrus FA			
L PLIC MD	0.362	0.328	0.268
L ALIC RD			
R precentral gyrus FA			
L lingual gyrus FA	0.378	0.345	0.267
R inferior frontal gyrus AD			
R parahippocampal gyrus AD			
R middle temporal gyrus FA	0.360	0.326	0.262
L inferior temporal gyrus RD			
R parahippocampal gyrus AD			

Table 5b

Classification of VLBW preterm infants at high-risk for gross motor impairment based on near-term regional white matter microstructure assessed on DTI, using exhaustive feature selection and logistic regression for prediction of BSID-III gross motor subscore below one standard deviation of the mean in preterm children at 18–22 months. The five most predictive set of three brain regions are listed.

Regions	AUC	Balanced		Maximum sensitivity		Maximum specificity	
		Sens	Spec	Sens	Spec	Sens	Spec
L lingual gyrus FA	0.84	0.933	0.667	1	0.467	0.2	1
R parahippocampal gyrus MD							
R gyrus rectus AD							
L lingual gyrus FA	0.837	0.867	0.756	1	0.444	0.067	1
R parahippocampal gyrus AD							
R lateral orbitofrontal gyrus AD							
L lingual gyrus FA	0.831	0.8	0.756	1	0.267	0.067	1
R parahippocampal gyrus AD							
R fusiform gyrus AD							
L lingual gyrus FA	0.831	0.8	0.778	0.933	0.6	0.333	1
R gyrus rectus AD							
R fornix MD							
L cuneus FA	0.828	0.8	0.733	1	0.489	0.133	1
L inferior temporal gyrus MD							
R fornix MD							

Individual patient DTI metrics of most predictive brain regions could be input into a simple spreadsheet to identify infants at high risk for cognitive and motor impairment.

Study limitations include the relatively small cohort that restricts the analysis to statistical tools that are less robust compared to state-of-the-art machine learning approaches, such as deep learning. In this study, we used linear models that have the advantage of easy interpretability and application to smaller sample sizes, however, in general, the solution space is highly nonlinear by nature; therefore, the achievable accuracy is limited compared to nonlinear models. In addition, assessment of cortical WM can be confounded by signal to noise ratio and imaging resolution. Methods employed in this study need to be repeated in a larger preterm population. Advances in neuroimaging methods will likely improve the prognostic values of machine learning based approaches.

Automated feature selection algorithms may allow for thorough analysis and identification of near-term regional neuronal microstructure most correlated with cognitive and motor development. Search in larger feature space may more accurately identify neonatal neural correlates of neurodevelopmental delay, and ultimately inform neuroprotective treatment to improve quality of life for preterm children. In this cohort, we used exhaustive feature search limited to finding a set of 3 regions that best predicted outcomes. Results indicate

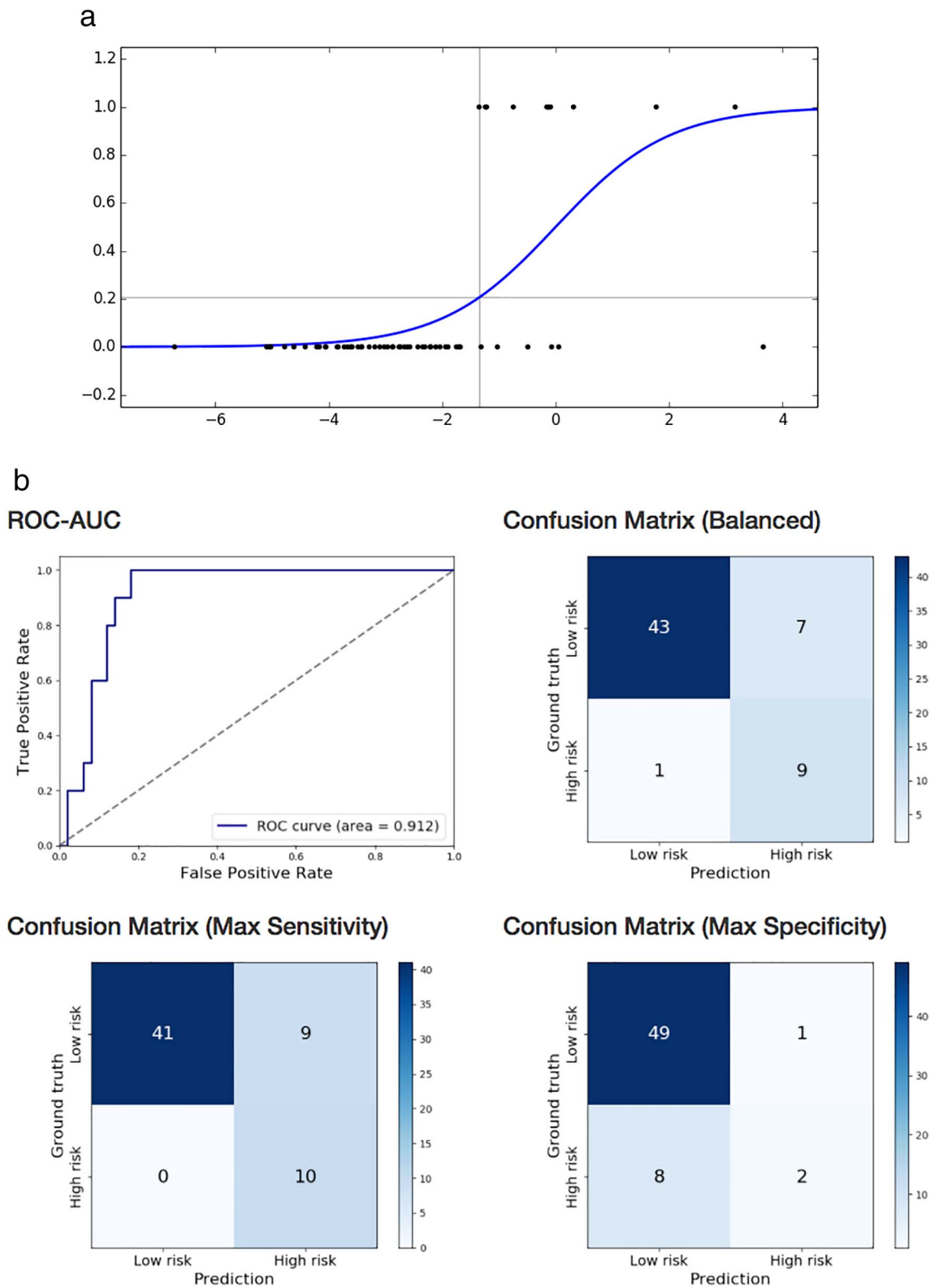


Fig. 2. a. Prediction of BSID-III motor composite score below one standard deviation of mean in preterm children at 18–22 months, based on near-term DTI using logistic regression. Logistic function fitted on left precuneus FA, right superior occipital gyrus MD, and right hippocampus FA. Score below one standard deviation of mean denoted by 1 on the y axis. b. Prediction of BSID-III motor composite score below one standard deviation of mean in preterm children at 18–22 months, based on near-term DTI using logistic regression. Receiver operating characteristics curve and confusion matrices of cross-validated classification of VLBW preterm infants at high-risk for motor impairment from left precuneus FA, right superior occipital gyrus MD, and right hippocampus FA.

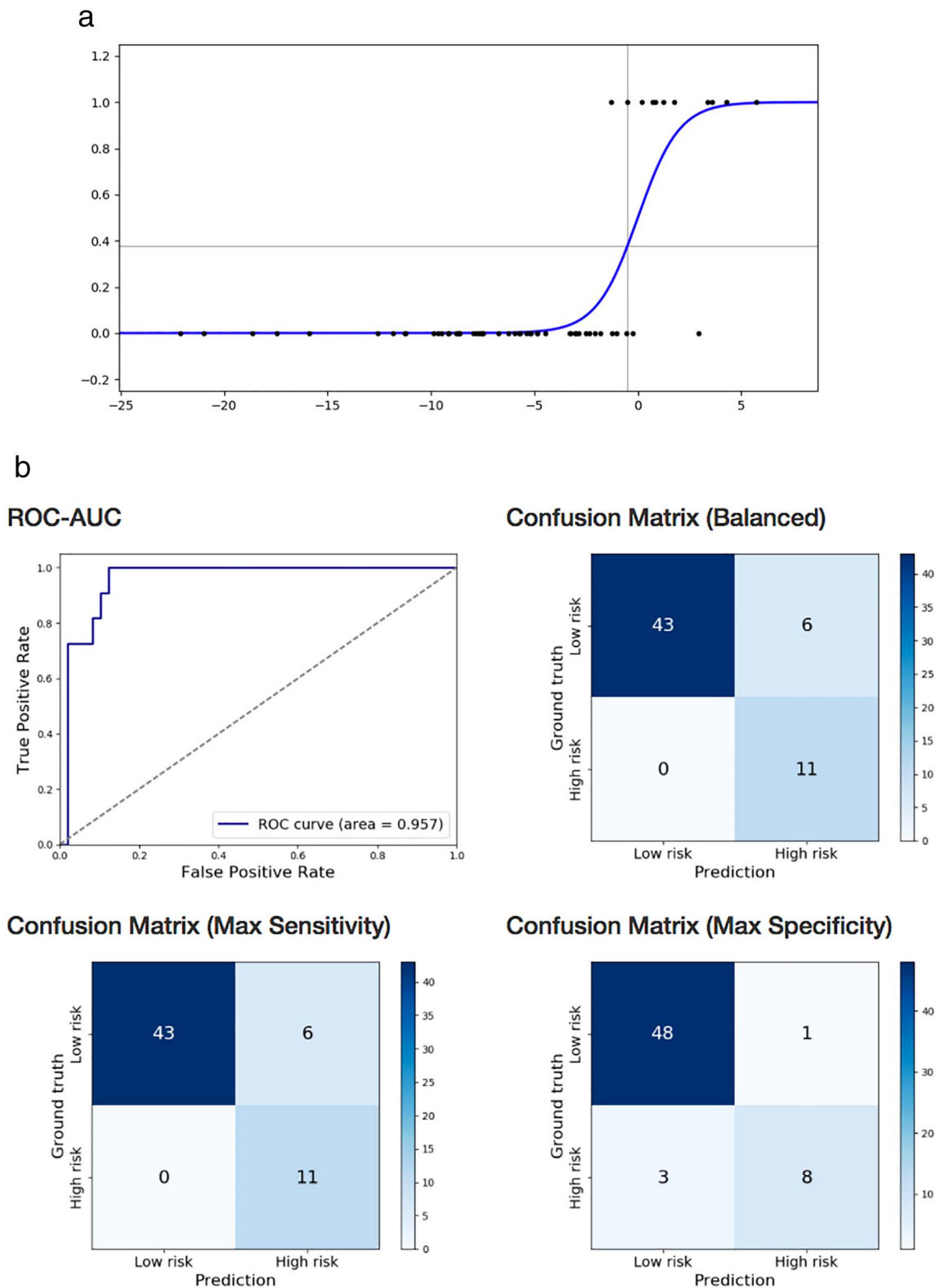


Fig. 3. a. Prediction of BSID-III fine motor subscore below one standard deviation of mean in preterm children at 18–22 months, based on near-term DTI using logistic regression. Logistic function fitted on left inferior occipital gyrus MD, right superior parietal gyrus MD, and right stria terminalis FA. Score below one standard deviation of the mean denoted by 1 on the y axis.

b. Prediction of BSID-III fine motor subscore below one standard deviation of mean in preterm children at 18–22 months, based on near-term DTI using logistic regression. Receiver operating characteristics curve and confusion matrices of cross-validated classification of VLBW preterm infants at high-risk for fine motor impairment from left inferior occipital gyrus MD, right superior parietal gyrus MD, and right stria terminalis FA.

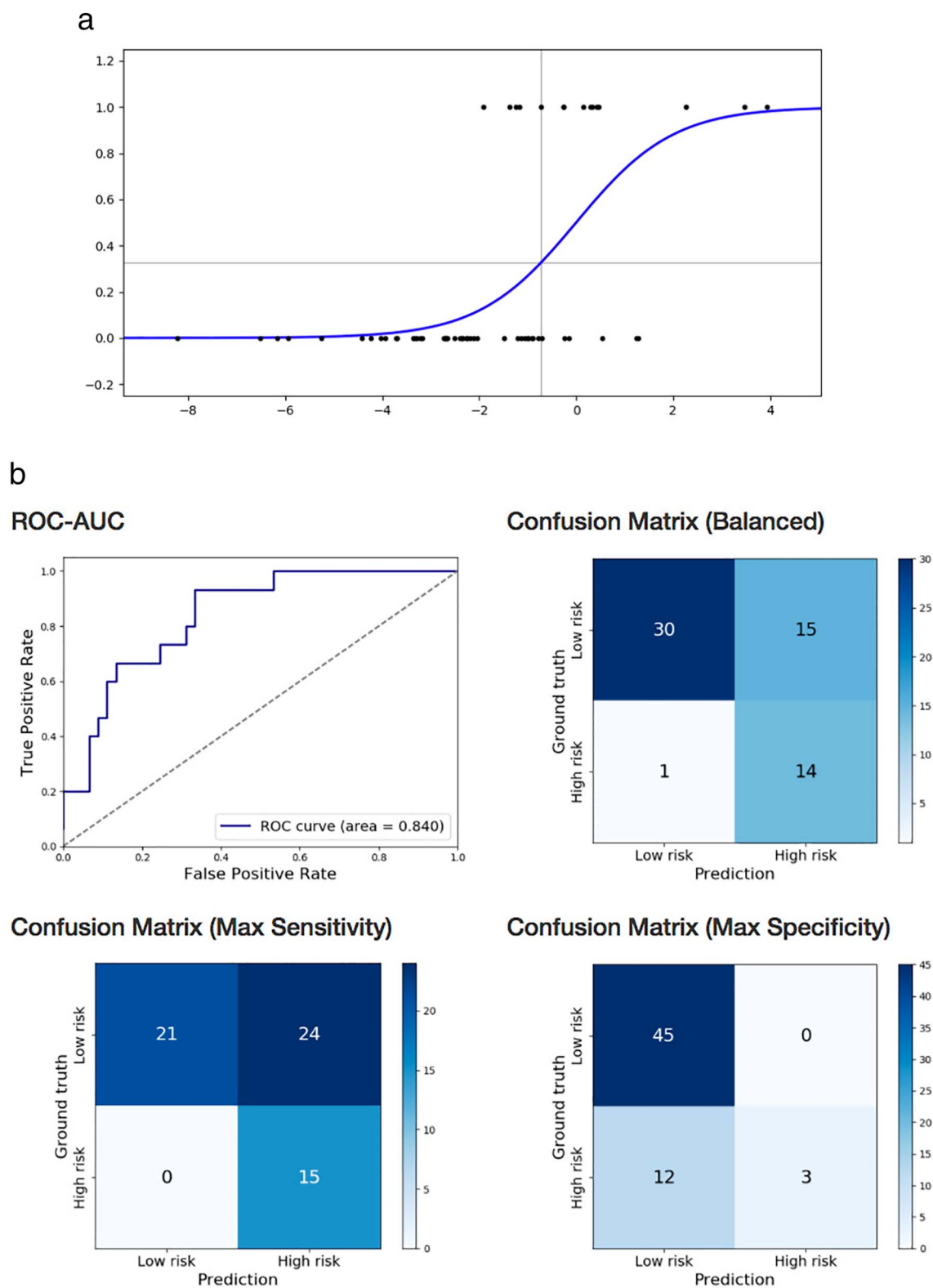


Fig. 4. a. Prediction of BSID-III gross motor subscore below one standard deviation of mean in preterm children at 18–22 months, based on near-term DTI using logistic regression. Logistic function fitted on left lingual gyrus FA, right gyrus rectus AD, and right parahippocampal gyrus MD. Score below one standard deviation of the mean denoted by 1 on the y axis. b. Prediction of BSID-III gross motor subscore below one standard deviation of mean in preterm children at 18–22 months, based on near-term DTI using logistic regression. Receiver operating characteristics curve and confusion matrices of cross-validated classification of VLBW preterm infants at high-risk for gross motor impairment from left lingual gyrus FA, right gyrus rectus AD, and right parahippocampal gyrus MD.

relatively high prognostic value for cognitive and motor development, and warrant further investigation in larger preterm populations.

Acknowledgments

We wish to thank Dr. Naama Barnea-Goraly, Dr. Susan Hintz, Dr. Ximena Stecher, Dr. John Tamaresis, Dr. Ron Cohen, Elizabeth Loi, and Dr. Megan Thompson for valuable discussions and assistance. This research was supported by the Chiesi Foundation, Parma Italy; NIH Clinical and Translational Science Award UL1 RR025744 for the Stanford Center for Clinical and Translational Education and Research (Spectrum) and for Stanford Center for Clinical Informatics, Stanford Translational Research Integrated Database Environment (STRIDE); Lucile Packard Foundation for Children's Health; NSF Graduate Research Fellowship grant no. DGE-1147470, and by the Mary Baracchi Research Fund, Lucile Packard Children's Hospital at Stanford. Authors have stated that they have no interests that might be perceived as posing a conflict or bias and there was no involvement of funders in the study design, data collection, analysis, article preparation or publication decisions.

References

- Aeby, A., De Tiège, X., Creuzil, M., David, P., Balériaux, D., Van Overmeire, B., Metens, T., Van Bogaert, P., 2013. Language development at 2 years is correlated to brain microstructure in the left superior temporal gyrus at term equivalent age: a diffusion tensor imaging study. *NeuroImage* 78, 145–151.
- Albouy, G., Sterpenich, V., Balteau, E., Vandewalle, G., Desseilles, M., Dang-Vu, T., Darsaud, A., Ruby, P., Luppi, P.-H., Degueldre, C., Peigneux, P., Luxen, A., Maquet, P., 2008. Both the hippocampus and striatum are involved in consolidation of motor sequence memory. *Neuron* 58, 261–272. <http://dx.doi.org/10.1016/j.neuron.2008.02.008>.
- Alvarez, R.P., Chen, G., Bodurka, J., Kaplan, R., Grillon, C., 2011. Phasic and sustained fear in humans elicits distinct patterns of brain activity. *NeuroImage* 55, 389–400.
- Arzoumanian, Y., Mirmiran, M., Barnes, P.D., Woolley, K., Ariagno, R.L., Moseley, M.E., Fleisher, B.E., Atlas, S.W., 2003. Diffusion tensor brain imaging findings at term-equivalent age may predict neurologic abnormalities in low birth weight preterm infants. *Am. J. Neuroradiol.* 24, 1646–1653.
- Barkovich, A.J., Kjos, B.O., Jackson Jr, D.E., Norman, D., 1988. Normal maturation of the neonatal and infant brain: MR imaging at 1.5 T. *Radiology* 166, 173–180.
- Basser, P.J., Pierpaoli, C., 2011. Microstructural and physiological features of tissues elucidated by quantitative-diffusion-tensor MRI. *J. Magn. Reson.* 213, 560–570.
- Brody, B.A., Kinney, H.C., Kloman, A.S., Gilles, F.H., 1987. Sequence of central nervous system myelination in human infancy. I. An autopsy study of myelination. *J. Neuropathol. Exp. Neurol.* 46, 283–301.
- Bruine, F.T., Wezel-Meijler, G., Leijser, L.M., Steggerda, S.J., Berg-Huysmans, D., Annette, A., Rijken, M., Buchem, M.A., Grond, J., 2013. Tractography of white-matter tracts in very preterm infants: a 2-year follow-up study. *Dev. Med. Child Neurol.* 55, 427–433.
- Bunge, S.A., Wright, S.B., 2007. Neurodevelopmental changes in working memory and cognitive control. *Curr. Opin. Neurobiol.* 17, 243–250.
- Cabeza, R., Nyberg, L., 2000. Imaging cognition II: an empirical review of 275 PET and fMRI studies. *J. Cogn. Neurosci.* 12, 1–47.
- Chao, L.L., Haxby, J.V., Martin, A., 1999. Attribute-based neural substrates in temporal cortex for perceiving and knowing about objects. *Nat. Neurosci.* 2.
- Counsell, S.J., Maalouf, E.F., Fletcher, A.M., Duggan, P., Battin, M., Lewis, H.J., Herlihy, A.H., Edwards, A.D., Bydder, G.M., Rutherford, M.A., 2002. MR imaging assessment of myelination in the very preterm brain. *Am. J. Neuroradiol.* 23, 872–881.
- Cowan, F.M., De Vries, L.S., 2005. The internal capsule in neonatal imaging. In: *Seminars in Fetal and Neonatal Medicine*. Elsevier, pp. 461–474.
- Devinsky, O., Morrell, M.J., Vogt, B.A., 1995. Contributions of anterior cingulate cortex to behaviour. *Brain* 118, 279–306.
- Dobbing, J., Sands, J., 1973. Quantitative growth and development of human brain. *Arch. Dis. Child.* 48, 757–767.
- Drobyshevsky, A., Bregman, J., Storey, P., Meyer, J., Prasad, P.V., Derrick, M., MacKendrick, W., Tan, S., 2007. Serial diffusion tensor imaging detects white matter changes that correlate with motor outcome in premature infants. *Dev. Neurosci.* 29, 289–301.
- Dubois, J., Hertz-Pannier, L., Dehaene-Lambertz, G., Cointepas, Y., Le Bihan, D., 2006. Assessment of the early organization and maturation of infants' cerebral white matter fiber bundles: a feasibility study using quantitative diffusion tensor imaging and tractography. *NeuroImage* 30, 1121–1132.
- Dubois, J., Dehaene-Lambertz, G., Perrin, M., Mangin, J.-F., Cointepas, Y., Duchesnay, E., Le Bihan, D., Hertz-Pannier, L., 2008. Asynchrony of the early maturation of white matter bundles in healthy infants: quantitative landmarks revealed noninvasively by diffusion tensor imaging. *Hum. Brain Mapp.* 29, 14–27.
- Finch, C.E., Randall, P.K., Marshall, J.F., 1981. Aging and basal ganglial functions. *Annu. Rev. Gerontol. Geriatr.* 2, 49–87.
- Fuster, J.M., 2002. Frontal lobe and cognitive development. *J. Neurocytol.* 31, 373–385.
- Gaillard, W.D., Pugliese, M., Grandin, C.B., Braniecki, S.H., Kondapaneni, P., Hunter, K., Xu, B., Petrella, J.R., Balsamo, L., Basso, G., 2001. Cortical localization of reading in normal children: an fMRI language study. *Neurology* 57, 47–54.
- Gimenez, M., Junque, C., Vendrell, P., Narberhaus, A., Bargallo, N., Botet, F., Mercader, J.M., 2006. Abnormal orbitofrontal development due to prematurity. *Neurology* 67, 1818–1822.
- Graybiel, A.M., 2000. The basal ganglia. *Curr. Biol.* 10, R509–511.
- Hanakawa, T., Immisch, I., Toma, K., Dimyan, M.A., Gelderen, P.V., Hallett, M., 2003. Functional properties of brain areas associated with motor execution and imagery. *J. Neurophysiol.* 89, 989–1002. <http://dx.doi.org/10.1152/jn.00132.2002>.
- Hastie, T., Tibshirani, R., Friedman, J., 2009. Overview of supervised learning. In: *The Elements of Statistical Learning*. Springer Series in Statistics. Springer, New York, NY, pp. 9–41. http://dx.doi.org/10.1007/978-0-387-84858-7_2.
- Herath, P., Kinomura, S., Roland, P.E., 2001. Visual recognition: evidence for two distinctive mechanisms from a PET study. *Hum. Brain Mapp.* 12, 110–119.
- Hintz, S.R., Barnes, P.D., Bulas, D., Slovis, T.L., Finer, N.N., Wraga, L.A., Das, A., Tyson, J.E., Stevenson, D.K., Carlo, W.A., et al., 2015. Neuroimaging and neurodevelopmental outcome in extremely preterm infants. *Pediatrics* 135, e32–e42.
- Horsch, S., Skiöld, B., Hallberg, B., Nordell, B., Nordell, A., Mosskin, M., Lagercrantz, H., Adén, U., Blennow, M., 2010. Cranial ultrasound and MRI at term age in extremely preterm infants. *Arch. Dis. Child. Fetal Neonatal Ed.* 95, F310–F314.
- Huang, H., Zhang, J., Wakana, S., Zhang, W., Ren, T., Richards, L.J., Yarowsky, P., Donohue, P., Graham, E., van Zijl, P.C., et al., 2006. White and gray matter development in human fetal, newborn and pediatric brains. *NeuroImage* 33, 27–38.
- Hüppi, P.S., Maier, S.E., Peled, S., Zientara, G.P., Barnes, P.D., Jolesz, F.A., Volpe, J.J., 1998. Microstructural development of human newborn cerebral white matter assessed in vivo by diffusion tensor magnetic resonance imaging. *Pediatr. Res.* 44, 584–590.
- Inder, T.E., Warfield, S.K., Wang, H., Hüppi, P.S., Volpe, J.J., 2005. Abnormal cerebral structure is present at term in premature infants. *Pediatrics* 115, 286–294.
- Isaacs, E.B., Edmonds, C.J., Chong, W.K., Lucas, A., Morley, R., Gadian, D.G., 2004. Brain morphology and IQ measurements in preterm children. *Brain* 127, 2595–2607.
- Ishai, A., Ungerleider, L.G., Martin, A., Schouten, J.L., Haxby, J.V., 1999. Distributed representation of objects in the human ventral visual pathway. *Proc. Natl. Acad. Sci.* 96, 9379–9384.
- Kesler, S.R., Ment, L.R., Vohr, B., Pajot, S.K., Schneider, K.C., Katz, K.H., Ebbitt, T.B., Duncan, C.C., Makuch, R.W., Reiss, A.L., 2004. Volumetric analysis of regional cerebral development in preterm children. *Pediatr. Neurol.* 31, 318–325.
- Kesler, S.R., Reiss, A.L., Vohr, B., Watson, C., Schneider, K.C., Katz, K.H., Maller-Kesselman, J., Silbereis, J., Constable, R.T., Makuch, R.W., et al., 2008. Brain volume reductions within multiple cognitive systems in male preterm children at age twelve. *J. Pediatr.* 152, 513–520.
- Kinney, H.C., Brody, B.A., Kloman, A.S., Gilles, F.H., 1988. Sequence of central nervous system myelination in human Infancy II. Patterns of myelination in autopsied infants. *J. Neuropathol. Exp. Neurol.* 47, 217–234. <http://dx.doi.org/10.1097/00005072-198805000-00003>.
- Kinney, H.C., Karthigasan, J., Borenshteyn, N.I., Flax, J.D., Kirschner, D.A., 1994. Myelination in the developing human brain: biochemical correlates. *Neurochem. Res.* 19, 983–996.
- Kontis, D., Catani, M., Cuddy, M., Walshe, M., Nosarti, C., Jones, D., Wyatt, J., Rifkin, L., Murray, R., Allin, M., 2009. Diffusion tensor MRI of the corpus callosum and cognitive function in adults born preterm. *Neuroreport* 20, 424–428.
- Krishnan, M.L., Dyet, L.E., Boardman, J.P., Kapellou, O., Allsop, J.M., Cowan, F., Edwards, A.D., Rutherford, M.A., Counsell, S.J., 2007. Relationship between white matter apparent diffusion coefficients in preterm infants at term-equivalent age and developmental outcome at 2 years. *Pediatrics* 120, e604–e609.
- Lee, A.Y., Jang, S.H., Lee, E., Ahn, S.H., Cho, H.K., Jo, H.M., Son, S.M., 2013. Radiologic differences in white matter maturation between preterm and full-term infants: TBSS study. *Pediatr. Radiol.* 43, 612–619.
- Liu, X.-B., Shen, Y., Plane, J.M., Deng, W., 2013. Vulnerability of premyelinating oligodendrocytes to white-matter damage in neonatal brain injury. *Neurosci. Bull.* 29, 229–238.
- Malik, S., Vinukonda, G., Vose, L.R., Diamond, D., Bhimavarapu, B.B., Hu, F., Zia, M.T., Hevner, R., Zecevic, N., Ballabh, P., 2013. Neurogenesis continues in the third trimester of pregnancy and is suppressed by premature birth. *J. Neurosci.* 33, 411–423.
- Miller, S.P., Ferriero, D.M., 2009. From selective vulnerability to connectivity: insights from newborn brain imaging. *Trends Neurosci.* 32, 496–505.
- Miyashita, Y., 1993. Inferior temporal cortex: where visual perception meets memory. *Annu. Rev. Neurosci.* 16, 245–263.
- Mukherjee, P., Miller, J.H., Shimony, J.S., Philip, J.V., Nehra, D., Snyder, A.Z., Conturo, T.E., Neil, J.J., McKinstry, R.C., 2002. Diffusion-tensor MR imaging of gray and white matter development during normal human brain maturation. *Am. J. Neuroradiol.* 23, 1445–1456.
- Nagy, Z., Westerberg, H., Skare, S., Andersson, J.L., Lilja, A., Flodmark, O., Fernell, E., Holmberg, K., Böhm, B., Forssberg, H., et al., 2003. Preterm children have disturbances of white matter at 11 years of age as shown by diffusion tensor imaging. *Pediatr. Res.* 54, 672–679.
- Nossin-Manor, R., Card, D., Morris, D., Noormohamed, S., Shroff, M.M., Whyte, H.E., Taylor, M.J., Sled, J.G., 2013. Quantitative MRI in the very preterm brain: assessing tissue organization and myelination using magnetization transfer, diffusion tensor and T1 imaging. *NeuroImage* 64, 505–516.
- Oishi, K., Mori, S., Donohue, P.K., Ernst, T., Anderson, L., Buchthal, S., Faria, A., Jiang, H., Li, X., Miller, M.I., et al., 2011. Multi-contrast human neonatal brain atlas: application to normal neonate development analysis. *NeuroImage* 56, 8–20.
- Pedregosa, F., Varoquaux, G., Gramfort, A., Michel, V., Thirion, B., Grisel, O., Blondel, M., Prettenhofer, P., Weiss, R., Dubourg, V., et al., 2011. Scikit-learn: machine learning in python. *J. Mach. Learn. Res.* 12, 2825–2830.

- Pierpaoli, C., Jezzard, P., Basser, P.J., Barnett, A., Di Chiro, G., 1996. Diffusion tensor MR imaging of the human brain. *Radiology* 201, 637–648.
- Rose, J., Mirmiran, M., Butler, E.E., Lin, C.Y., Barnes, P.D., Kermoian, R., Stevenson, D.K., 2007. Neonatal microstructural development of the internal capsule on diffusion tensor imaging correlates with severity of gait and motor deficits. *Dev. Med. Child Neurol.* 49, 745–750.
- Rose, S.E., Hatzigeorgiou, X., Strudwick, M.W., Durbridge, G., Davies, P.S., Colditz, P.B., 2008. Altered white matter diffusion anisotropy in normal and preterm infants at term-equivalent age. *Magn. Reson. Med.* 60, 761–767.
- Rose, J., Butler, E.E., Lamont, L.E., Barnes, P.D., Atlas, S.W., Stevenson, D.K., 2009. Neonatal brain structure on MRI and diffusion tensor imaging, sex, and neurodevelopment in very-low-birthweight preterm children. *Dev. Med. Child Neurol.* 51, 526–535.
- Rose, J., Vassar, R., Cahill-Rowley, K., Guzman, X.S., Stevenson, D.K., Barnea-Goraly, N., 2014. Brain microstructural development at near-term age in very-low-birth-weight preterm infants: an atlas-based diffusion imaging study. *NeuroImage* 86, 244–256.
- Rose, J., Cahill-Rowley, K., Vassar, R., Yeom, K.W., Stecher, X., Stevenson, D.K., Hintz, S.R., Barnea-Goraly, N., 2015. Neonatal brain microstructure correlates of neurodevelopment and gait in preterm children 18–22 mo of age: an MRI and DTI study. *Pediatr. Res.* 78, 700–708.
- Schmahmann, J.D., Pandya, D.N., Wang, R., Dai, G., D'arceuil, H.E., de Crespigny, A.J., Wedeen, V.J., 2007. Association fibre pathways of the brain: parallel observations from diffusion spectrum imaging and autoradiography. *Brain* 130, 630–653.
- Seabold, S., Perktold, J., 2010. Statsmodels: econometric and statistical modeling with python. In: *Proceedings of the 9th Python in Science Conference*, pp. 61.
- Serag, A., Aljabar, P., Ball, G., Counsell, S.J., Boardman, J.P., Rutherford, M.A., Edwards, A.D., Hajnal, J.V., Rueckert, D., 2012. Construction of a consistent high-definition spatio-temporal atlas of the developing brain using adaptive kernel regression. *NeuroImage* 59, 2255–2265.
- Short, S.J., Elison, J.T., Goldman, B.D., Styner, M., Gu, H., Connelly, M., Maltbie, E., Woolson, S., Lin, W., Gerig, G., et al., 2013. Associations between white matter microstructure and infants' working memory. *NeuroImage* 64, 156–166.
- Snook, L., Paulson, L.-A., Roy, D., Phillips, L., Beaulieu, C., 2005. Diffusion tensor imaging of neurodevelopment in children and young adults. *NeuroImage* 26, 1164–1173.
- Spittle, A.J., Cheong, J., Doyle, L.W., Roberts, G., Lee, K.J., Lim, J., Hunt, R.W., Inder, T.E., Anderson, P.J., 2011. Neonatal white matter abnormality predicts childhood motor impairment in very preterm children. *Dev. Med. Child Neurol.* 53, 1000–1006.
- Suchan, B., Yáñez, L., Wunderlich, G., Canavan, A.G.M., Herzog, H., Tellmann, L., Hömberg, V., Seitz, R.J., 2002. Hemispheric dissociation of visual-pattern processing and visual rotation. *Behav. Brain Res.* 136, 533–544. [http://dx.doi.org/10.1016/S0166-4328\(02\)00204-8](http://dx.doi.org/10.1016/S0166-4328(02)00204-8).
- Thompson, D.K., Warfield, S.K., Carlin, J.B., Pavlovic, M., Wang, H.X., Bear, M., Kean, M.J., Doyle, L.W., Egan, G.F., Inder, T.E., 2006. Perinatal risk factors altering regional brain structure in the preterm infant. *Brain* 130, 667–677.
- Thompson, D.K., Adamson, C., Roberts, G., Faggian, N., Wood, S.J., Warfield, S.K., Doyle, L.W., Anderson, P.J., Egan, G.F., Inder, T.E., 2013. Hippocampal shape variations at term equivalent age in very preterm infants compared with term controls: perinatal predictors and functional significance at age 7. *NeuroImage* 70, 278–287.
- Tranel, D., Damasio, H., Damasio, A.R., 1997. A neural basis for the retrieval of conceptual knowledge. *Neuropsychologia* 35, 1319–1327.
- Tsao, H., Pannek, K., Fiori, S., Boyd, R., Rose, S., 2014. Reduced integrity of sensorimotor projections traversing the posterior limb of the internal capsule in children with congenital hemiparesis. *Res. Dev. Disabil.* 35, 250–260.
- Van Kooij, B.J., van Pul, C., Benders, M.J., van Haastert, I.C., de Vries, L.S., Groenendaal, F., 2011. Fiber tracking at term displays gender differences regarding cognitive and motor outcome at 2 years of age in preterm infants. *Pediatr. Res.* 70, 626–632.
- Vangberg, T.R., Skranes, J., Dale, A.M., Martinussen, M., Brubakk, A.-M., Haraldseth, O., 2006. Changes in white matter diffusion anisotropy in adolescents born prematurely. *NeuroImage* 32, 1538–1548.
- Wang, L., Wang, Y., Chang, Q., 2016. Feature selection methods for big data bioinformatics: a survey from the search perspective. *Methods* 111, 21–31. (Big Data Bioinformatics). <https://doi.org/10.1016/j.ymeth.2016.08.014>.
- Wenderoth, N., Debaere, F., Sunaert, S., Swinnen, S.P., 2005. The role of anterior cingulate cortex and precuneus in the coordination of motor behaviour. *Eur. J. Neurosci.* 22, 235–246. <http://dx.doi.org/10.1111/j.1460-9568.2005.04176.x>.
- Williams, J., Lee, K.J., Anderson, P.J., 2010. Prevalence of motor-skill impairment in preterm children who do not develop cerebral palsy: a systematic review. *Dev. Med. Child Neurol.* 52, 232–237.
- Woodward, L.J., Anderson, P.J., Austin, N.C., Howard, K., Inder, T.E., 2006. Neonatal MRI to predict neurodevelopmental outcomes in preterm infants. *N. Engl. J. Med.* 355, 685–694.
- Woodward, L.J., Clark, C.A., Bora, S., Inder, T.E., 2012. Neonatal white matter abnormalities an important predictor of neurocognitive outcome for very preterm children. *PLoS One* 7, e51879.
- Yakovlev, P.I., 1967. The myelogenic cycles of regional maturation of the brain. In: *Regional Dev. Brain Early Life*, pp. 3–70.